

DOI: 10.1002/ange.200601060

# Experimental Evidence for Linear Metal–Azido Coordination: The Binary Group 5 Azides $[\text{Nb}(\text{N}_3)_5]$ , $[\text{Ta}(\text{N}_3)_5]$ , $[\text{Nb}(\text{N}_3)_6]^-$ , and $[\text{Ta}(\text{N}_3)_6]^-$ , and 1:1 Acetonitrile Adducts $[\text{Nb}(\text{N}_3)_5(\text{CH}_3\text{CN})]$ and $[\text{Ta}(\text{N}_3)_5(\text{CH}_3\text{CN})]$ \*\*

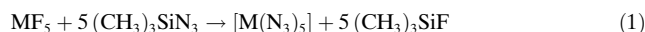
Ralf Haiges,\* Jerry A. Boatz, Thorsten Schroer, Muhammed Yousufuddin, and Karl O. Christe\*

Dedicated to Professor Reint Eujen  
on the occasion of his 60th birthday

Whereas the existence of numerous binary transition-metal–azido complexes has been reported,<sup>[1–3]</sup> no binary Group 5 azides are known. Only a limited number of partially azido-substituted compounds of vanadium, niobium, and tantalum have previously been reported.<sup>[4–21]</sup>

Herein, we communicate the synthesis and characterization of  $[\text{Nb}(\text{N}_3)_5]$ ,  $[\text{Ta}(\text{N}_3)_5]$ , and their 1:1 adducts with  $\text{CH}_3\text{CN}$ , as well as the anions  $[\text{Nb}(\text{N}_3)_6]^-$  and  $[\text{Ta}(\text{N}_3)_6]^-$ . The crystal structures of  $[\text{Nb}(\text{N}_3)_5(\text{CH}_3\text{CN})]$  and  $[\text{PPh}_4][\text{Nb}(\text{N}_3)_6]$  and the first experimental evidence for the existence of azido compounds with linear M–N–N coordination are also reported.

The reactions of  $\text{NbF}_5$  or  $\text{TaF}_5$  with excess  $(\text{CH}_3)_3\text{SiN}_3$  in  $\text{SO}_2$  solution at  $-20^\circ\text{C}$  resulted in complete fluorido–azido exchange and yielded clear solutions of  $[\text{Nb}(\text{N}_3)_5]$  or  $[\text{Ta}(\text{N}_3)_5]$ , respectively [Eq. (1) ( $\text{M} = \text{Nb}, \text{Ta}$ )].



When the volatile compounds ( $\text{SO}_2$ ,  $(\text{CH}_3)_3\text{SiF}$ , and excess  $(\text{CH}_3)_3\text{SiN}_3$ ) were removed in a vacuum at  $-20^\circ\text{C}$ , pure, yellow, solid, room-temperature-stable pentaazido complexes were produced in quantitative yield. As expected for covalently bonded polyazido complexes,<sup>[22]</sup> they are shock-sensitive and can explode violently when touched with a metal spatula or by heating in the flame of a Bunsen burner. Their identity was established by the observed mass balances, vibrational spectroscopy, and their conversions with  $\text{N}_3^-$  into hexaazido metalates and with  $\text{CH}_3\text{CN}$  into 1:1 acetonitrile donor–acceptor adducts, as shown by the crystal structures of  $[\text{P}(\text{C}_6\text{H}_5)_4]^+[\text{Nb}(\text{N}_3)_6]^-$  and  $[\text{Nb}(\text{N}_3)_5(\text{CH}_3\text{CN})]$ .

The observed IR and Raman spectra of  $[\text{Nb}(\text{N}_3)_5]$  and  $[\text{Ta}(\text{N}_3)_5]$  are shown in the Supporting Information, and the observed frequencies and intensities are listed in the Experimental Section. These data were assigned by comparison with those calculated at the B3LYP<sup>[23]</sup> and MP2<sup>[24]</sup> levels of theory by using SBKJ + (d) basis sets.<sup>[25]</sup> The agreement between the observed and calculated spectra is satisfactory and supports the existence of trigonal-bipyramidal structures (Table 1) for  $[\text{Nb}(\text{N}_3)_5]$  and  $[\text{Ta}(\text{N}_3)_5]$ . The internal vibrational modes of the azido ligands are split into clusters of five as a result of in-phase and out-of-phase coupling of the individual motions. There are always one in-phase and four out-of-phase vibrations, with the in-phase vibration readily identifiable from its higher Raman intensity. The  $\text{MN}_5$  skeletal modes can be derived from  $D_{3h}$  symmetry in which the double degeneracy of the E modes is lifted as a result of the presence of the azido ligands, which lowers the overall symmetry to  $C_s$  and is likely to produce some distortion from  $D_{3h}$  symmetry.

Whereas trigonal-bipyramidal arrangements of the azido ligands have previously also been found for  $[\text{Fe}(\text{N}_3)_5]^{2-}$ <sup>[26]</sup> and theoretically predicted for  $[\text{Sb}(\text{N}_3)_5]$  and  $[\text{As}(\text{N}_3)_5]$ ,<sup>[27,28]</sup> the details of these structures are very different. In  $[\text{Fe}(\text{N}_3)_5]^{2-}$ ,  $[\text{As}(\text{N}_3)_5]$ , and  $[\text{Sb}(\text{N}_3)_5]$ , all five M–N–N units are strongly bent, and the two axial M–N bonds are significantly longer than the equatorial ones, as expected from VSEPR arguments.<sup>[29]</sup> In contrast, the axial M–N–N arrangements in  $[\text{Nb}(\text{N}_3)_5]$  and  $[\text{Ta}(\text{N}_3)_5]$  are calculated to be almost linear, while the equatorial ones have calculated angles of about  $137^\circ$ . Furthermore, all five M–N bond lengths and the internal N–N bond lengths of the five azido ligands are essentially the same in each compound.

Linear M–N–N coordination had previously been predicted also for the tetraazido complexes of the  $d^0$  centers  $\text{Ti}^{\text{IV}}$ ,  $\text{Zr}^{\text{IV}}$ , and  $\text{Hf}^{\text{IV}}$ ,<sup>[30]</sup> as well as for the  $d^6$   $\text{Fe}^{\text{II}}$  center,<sup>[31]</sup> but the hexaazido dianion of the  $d^0$   $\text{Ti}^{\text{IV}}$  center was shown experimentally to possess strongly bent Ti–N–N units.<sup>[1]</sup> These findings show that the linearity of the M–N–N units cannot be caused by either a trigonal-bipyramidal structure, multiple M–N bonds, or a  $d^0$  electronic configuration per se.

The occurrence of linear M–N–N groups can be predicted by theoretical calculations.<sup>[30,31]</sup> A plausible explanation for the linearity of these M–N–N groups has recently been given,<sup>[1]</sup> as based on an analogy with the known crystal structure of  $[\text{Zr}(\text{BH}_4)_4]$ .<sup>[32]</sup> A tentative model was proposed in which the  $\text{N}_\alpha$  atoms of the azido ligands act as tridative<sup>[1]</sup> ligands.

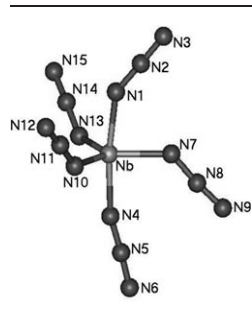
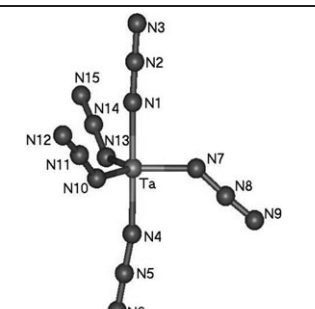
[\*] Dr. R. Haiges, Dr. T. Schroer, Dr. M. Yousufuddin, Prof. Dr. K. O. Christe  
Loker Research Institute and Department of Chemistry  
University of Southern California  
Los Angeles, CA 90089-1661 (USA)  
Fax: (+1) 213-740-6679  
E-mail: haiges@usc.edu  
kchriste@usc.edu

Dr. J. A. Boatz  
Space and Missile Propulsion Division  
Air Force Research Laboratory (AFRL/PRSP)  
10 East Saturn Boulevard, Bldg 8451  
Edwards Air Force Base, CA 93524 (USA)

[\*\*] This work was funded by the Air Force Office of Scientific Research and the National Science Foundation. We thank Prof. Dr. G. A. Olah and Dr. M. Berman for their steady support, and Prof. D. Dixon, Prof. Dr. R. Bau, Drs. R. Wagner and W. W. Wilson, and C. Bigler Jones for their help and stimulating discussions. We gratefully acknowledge grants of computer time at the Aeronautical Systems Center (Wright–Patterson Air Force Base, Dayton, OH), the Naval Oceanographic Office (Stennis Space Center, MS), the Engineer Research and Development Center (Vicksburg, MS), the Army Research Laboratory (Aberdeen Proving Ground, MD), and the Army High Performance Computing Research Center (Minneapolis, MN), under sponsorship of the Department of Defense High Performance Computing Modernization Program Office.

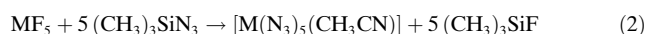
Supporting information for this article is available on the WWW under <http://www.angewandte.org> or from the author.

**Table 1:** Calculated structures of  $[\text{Nb}(\text{N}_3)_5]$  and  $[\text{Ta}(\text{N}_3)_5]$  at the B3LYP/SBKJ + (d) level of theory (MP2/SBKJ + (d) values in parentheses).

			
Bond lengths [Å]		Bond lengths [Å]	
Nb-N1	2.025 (2.013)	Ta-N1	1.997 (1.996)
Nb-N4	2.001 (2.002)	Ta-N4	1.991 (1.993)
Nb-N7	2.048 (2.060)	Ta-N7	2.003 (1.997)
Nb-N10	2.008 (2.014)	Ta-N10	2.008 (2.009)
Nb-N13	2.008 (2.014)	Ta-N13	2.008 (2.009)
N1-N2	1.234 (1.241)	N1-N2	1.226 (1.235)
N4-N5	1.230 (1.241)	N4-N5	1.225 (1.234)
N7-N8	1.243 (1.249)	N7-N8	1.240 (1.242)
N10-N11	1.240 (1.245)	N10-N11	1.240 (1.244)
N13-N14	1.240 (1.245)	N13-N14	1.240 (1.244)
N2-N3	1.162 (1.208)	N2-N3	1.163 (1.209)
N5-N6	1.163 (1.210)	N5-N6	1.163 (1.209)
N8-N9	1.162 (1.210)	N8-N9	1.160 (1.206)
N11-N12	1.160 (1.208)	N11-N12	1.160 (1.206)
N14-N15	1.160 (1.208)	N14-N15	1.160 (1.206)
Bond angles [°]		Bond angles [°]	
N1-Nb-N4	171.9 (169.0)	N1-Ta-N4	179.2 (177.9)
N1-Nb-N7	82.8 (81.4)	N1-Ta-N7	89.4 (90.2)
N1-Nb-N10	91.0 (92.1)	N1-Ta-N10	90.2 (89.8)
N1-Nb-N13	91.0 (92.1)	N1-Ta-N13	90.2 (89.8)
N4-Nb-N7	89.1 (87.6)	N4-Ta-N7	91.4 (91.8)
N4-Nb-N10	93.2 (93.6)	N4-Ta-N10	89.4 (89.2)
N4-Nb-N13	93.2 (93.6)	N4-Ta-N13	89.4 (89.2)
N7-Nb-N10	121.3 (121.3)	N7-Ta-N10	119.6 (119.1)
N7-Nb-N13	121.3 (121.3)	N7-Ta-N13	119.6 (119.1)
N10-Nb-N13	117.2 (117.1)	N10-Ta-N13	120.9 (121.7)
Nb-N1-N2	145.3 (147.2)	Ta-N1-N2	176.9 (178.5)
Nb-N4-N5	165.0 (157.3)	Ta-N4-N5	169.3 (173.8)
Nb-N7-N8	131.8 (130.8)	Ta-N7-N8	137.7 (143.0)
Nb-N10-N11	137.2 (138.8)	Ta-N10-N11	137.1 (138.9)
Nb-N13-N14	137.2 (138.8)	Ta-N13-N14	137.1 (138.9)

However, this explanation might be incorrect, and a detailed analysis of the occurrence of linear M-N-N configurations in the periodic system and of the nature of the bonds involved is presently being carried out by us and will be the subject of a future publication.

By using  $\text{CH}_3\text{CN}$  instead of  $\text{SO}_2$  as a solvent for the reactions of  $\text{NbF}_5$  and  $\text{TaF}_5$  with excess  $(\text{CH}_3)_3\text{SiN}_3$ , yellow solutions of  $[\text{Nb}(\text{N}_3)_5(\text{CH}_3\text{CN})]$  and  $[\text{Ta}(\text{N}_3)_5(\text{CH}_3\text{CN})]$ , respectively, were obtained [Eq. (2) ( $\text{M} = \text{Nb}, \text{Ta}$ )].



Removal of the volatile compounds ( $\text{CH}_3\text{CN}$ ,  $(\text{CH}_3)_3\text{SiF}$ , and excess  $(\text{CH}_3)_3\text{SiN}_3$ ) at  $-20^\circ\text{C}$  resulted in the isolation of the acetonitrile adducts of the pentaazido complexes.

Although still dangerous and explosive, both acetonitrile adducts are less shock-sensitive than the corresponding donor-free complexes.

Both acetonitrile adducts were isolated as yellow solids and were characterized by vibrational spectroscopy, their conversions with  $\text{N}_3^-$  into the hexaazido metalates, and, in the case of  $[\text{Nb}(\text{N}_3)_5(\text{CH}_3\text{CN})]$ , by its crystal structure.<sup>[33]</sup> The observed Raman spectra of  $[\text{Nb}(\text{N}_3)_5(\text{CH}_3\text{CN})]$  and  $[\text{Ta}(\text{N}_3)_5(\text{CH}_3\text{CN})]$  are shown in Figure 1 and in the Supporting

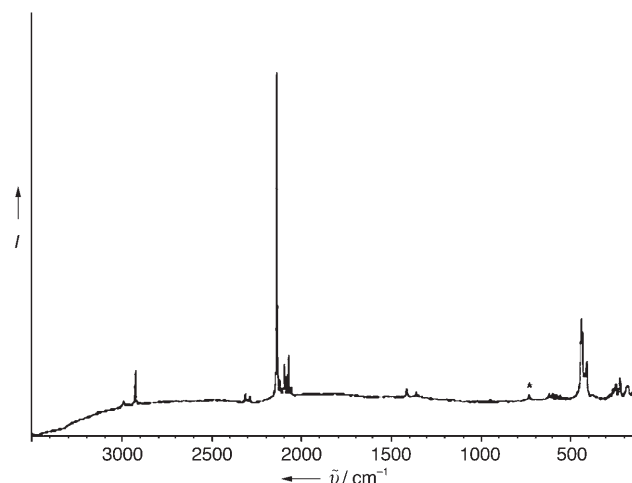


**Figure 1.** Raman spectrum of solid  $[\text{Nb}(\text{N}_3)_5(\text{CH}_3\text{CN})]$ . The band marked by an asterisk (\*) is from the teflon-FEP sample tube.

Information, respectively, and their frequencies and intensities are given in the Experimental Section. A comparison with the calculated spectra is given in the Supporting Information, and the given assignments are in accord with those previously reported<sup>[34,35]</sup> for the related  $[\text{SbF}_5(\text{CH}_3\text{CN})]$  adduct.

$[\text{Nb}(\text{N}_3)_5(\text{CH}_3\text{CN})]$  crystallizes in the monoclinic space group  $P2_1/c$ . The X-ray structure analysis<sup>[33]</sup> (Figure 2) reveals the presence of isolated  $[\text{Nb}(\text{N}_3)_5(\text{CH}_3\text{CN})]$  units. The closest intermolecular  $\text{Nb} \cdots \text{N}$  and  $\text{N} \cdots \text{N}$  contacts are 3.98 Å and 3.04 Å, respectively. The molecule consists of a pseudo-octahedral  $\text{NbN}_6$  skeleton with the  $\text{CH}_3\text{CN}$  ligand and one azido ligand in the axial positions. The equatorial positions are occupied by the remaining four azido ligands, which, interestingly, are all bent away from the axial azido ligand. The axial  $\text{Nb}-\text{N}_{\text{azido}}$  bond length is about 0.09 Å shorter than the four equatorial ones. The most interesting feature, however, is the fact that the axial azido ligand exhibits a large  $\text{Nb}-\text{N}-\text{N}$  bond angle of  $168.8(3)^\circ$ , compared to an average angle of  $137.8^\circ$  for the four equatorial ligands. The small deviation of the observed axial  $\text{Nb}-\text{N}-\text{N}$  bond angle from  $180^\circ$  is attributed to solid-state effects, as our theoretical calculations for the free gaseous molecule at the B3LYP and MP2 levels of theory with an SBKJ + (d) basis set resulted in  $\text{Nb}-\text{N}-\text{N}$  bond angles of  $179.6^\circ$  and  $178.3^\circ$ , respectively. For free  $[\text{Ta}(\text{N}_3)_5(\text{CH}_3\text{CN})]$ , analogous calculations gave  $\text{Ta}-\text{N}-\text{N}$  bond angles of  $179.6^\circ$  and  $180.0^\circ$ . The significant shortening of the axial  $\text{Nb}-\text{N}_{\text{azido}}$  bond length can be attributed to a *trans* effect that is caused by the long  $\text{Nb}-\text{NCCCH}_3$  bond.

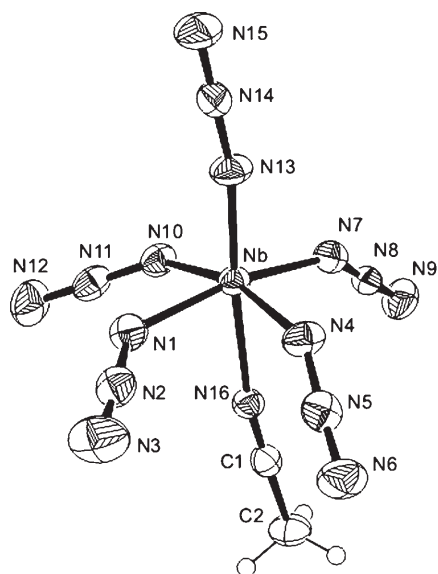
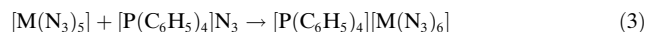


**Figure 2.** ORTEP plot of  $[\text{Nb}(\text{N}_3)_5(\text{CH}_3\text{CN})]$ . Thermal ellipsoids are shown at the 50% probability level. Selected bond lengths [Å] and angles [°]: Nb–N1 2.031(3), Nb–N4 1.998(3), Nb–N7 2.004(3), Nb–N10 2.017(3), Nb–N13 1.935(3), Nb–N16 2.259(3), N1–N2 1.217(4), N2–N3 1.139(4), N4–N5 1.212(4), N5–N6 1.133(4), N7–N8 1.212(4), N8–N9 1.129(4), N10–N11 1.211(4), N11–N12 1.132(4), N13–N14 1.205(4), N14–N15 1.137(4), N16–C1 1.139(4), C1–C2 1.447(5); N1–Nb–N4 87.55(12), N1–Nb–N7 165.51(11), N1–Nb–N10 82.89(12), N1–Nb–N13 99.16(12), N1–Nb–N16 84.59(10), N4–Nb–N7 93.90(12), N4–Nb–N10 162.91(12), N4–Nb–N13 96.38(12), N4–Nb–N16 81.15(10), N7–Nb–N10 91.93(11), N7–Nb–N13 95.01(12), N7–Nb–N16 81.40(11), N10–Nb–N13 99.11(12), N10–Nb–N16 83.86(10), N13–Nb–N16 175.45(11), Nb–N1–N2 132.7(2), Nb–N4–N5 141.9(2), Nb–N7–N8 144.1(2), Nb–N10–N11 132.3(2), Nb–N13–N14 168.8(3), Nb–N16–C1 170.6(3).

The average Nb–N<sub>azido</sub> bond length of 1.997 Å in  $[\text{Nb}(\text{N}_3)_5(\text{CH}_3\text{CN})]$  is significantly smaller than those found for the terminal azido ligands of two isomers of  $[\text{Cp}^*\text{NbCl}(\text{N}_3)(\mu\text{-N}_3)_2(\mu\text{-O})]^{[16]}$  (2.081 Å and 2.105 Å) and that found for the cluster  $[\text{Nb}_6\text{Br}_{12}(\text{N}_3)_6]^{4-}$ <sup>[18]</sup> (2.27 Å), but slightly longer than that found in  $[\text{NbCl}_5(\text{N}_3)]^{-}$ <sup>[19]</sup> (1.92 Å), and is attributed to varying degrees of ionicity of the azido ligands in these compounds.

The reactions of the pentaazido complexes with ionic azides, such as  $[\text{P}(\text{C}_6\text{H}_5)_4]^+\text{N}_3^-$ , in  $\text{CH}_3\text{CN}$  solution produced the corresponding  $[\text{Nb}(\text{N}_3)_6]^-$  and  $[\text{Ta}(\text{N}_3)_6]^-$  salts [Eq. (3) ( $\text{M} = \text{Nb}, \text{Ta}$ )].



The hexaazido niobates and tantalates were isolated as yellow-orange solids and are stable at room temperature. The compounds were characterized by the observed mass balances, vibrational spectroscopy, and, in the case of  $[\text{P}(\text{C}_6\text{H}_5)_4][\text{Nb}(\text{N}_3)_6]$ , by its crystal structure.<sup>[36]</sup> The observed vibrational spectra of  $[\text{P}(\text{C}_6\text{H}_5)_4][\text{Nb}(\text{N}_3)_6]$  and  $[\text{P}(\text{C}_6\text{H}_5)_4][\text{Ta}(\text{N}_3)_6]$  are shown in the Supporting Information, and their frequencies and intensities are given in Table 2 ( $[\text{Nb}(\text{N}_3)_6]^-$ ) and in the Experimental Section ( $[\text{Ta}(\text{N}_3)_6]^-$ ). The free  $[\text{Nb}(\text{N}_3)_6]^-$  anion is predicted to have perfect  $S_6$  ( $\equiv C_{3i}$ ) symmetry in the gas phase, which is quite rare,<sup>[37]</sup> and, therefore, a complete

vibrational analysis was carried out (Table 2).  $[\text{Ta}(\text{N}_3)_6]^-$  is slightly distorted from  $S_6$  to  $C_1$  symmetry, but its structure is almost identical to that of  $[\text{Nb}(\text{N}_3)_6]^-$ , and the splittings of its degenerate vibrational modes are extremely small (Supporting Information).

Because of the presence of a large counterion, which serves as an inert spacer and suppresses detonation propagation, these salts are much less shock-sensitive than  $[\text{Nb}(\text{N}_3)_5]$  and  $[\text{Ta}(\text{N}_3)_5]$ , and are thermally surprisingly stable. Single crystals of  $[\text{P}(\text{C}_6\text{H}_5)_4][\text{Nb}(\text{N}_3)_6]$  were obtained by recrystallization from  $\text{CH}_3\text{CN}$ . The salt crystallizes in the rare orthorhombic space group  $P2_12_12$ . The X-ray structure analysis<sup>[36]</sup> of  $[\text{P}(\text{C}_6\text{H}_5)_4][\text{Nb}(\text{N}_3)_6]$  (Figure 3) reveals no significant

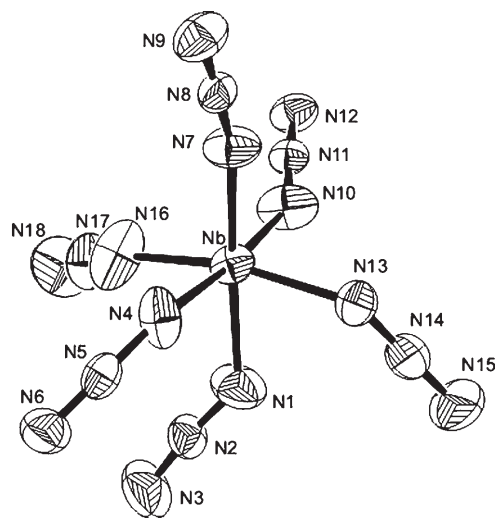


**Figure 3.** ORTEP plot of the anion in the crystal structure of  $[\text{P}(\text{C}_6\text{H}_5)_4][\text{Nb}(\text{N}_3)_6]$ . Thermal ellipsoids are shown at the 50% probability level. Selected bond lengths [Å] and angles [°]: Nb–N1 2.078(5), Nb–N4 2.035(4), Nb–N7 1.989(4), Nb–N10 2.008(4), Nb–N13 2.032(4), Nb–N16 2.026(5), N1–N2 1.164(5), N2–N3 1.126(6), N4–N5 1.198(5), N5–N6 1.128(5), N7–N8 1.192(5), N8–N9 1.133(5), N10–N11 1.196(5), N11–N12 1.118(5), N13–N14 1.203(6), N14–N15 1.137(6), N16–N17 1.173(6), N17–N18 1.137(6); N1–Nb–N4 89.54(19), N1–Nb–N7 173.25(18), N1–Nb–N10 94.23(18), N1–Nb–N13 80.45(18), N1–Nb–N16 85.2(2), N4–Nb–N7 86.30(18), N4–Nb–N10 174.15(18), N4–Nb–N13 95.40(15), N4–Nb–N16 86.78(17), N7–Nb–N10 90.34(17), N7–Nb–N13 94.63(17), N7–Nb–N16 99.86(19), N10–Nb–N13 89.63(18), N10–Nb–N16 89.1(2), N13–Nb–N16 165.46(18), Nb–N1–N2 134.4(4), Nb–N4–N5 141.2(4), Nb–N7–N8 156.2(4), Nb–N10–N11 152.3(4), Nb–N13–N14 131.7(4), Nb–N16–N17 142.3(4).

cation–anion and anion–anion interactions. The closest intermolecular Nb⋯N and N⋯N contacts are 4.20 Å and 3.15 Å, respectively. The structure of the  $[\text{Nb}(\text{N}_3)_6]^-$  anion in the solid state is distorted from the perfect  $S_6$  symmetry that was predicted by our theoretical calculations for the free anion in the gas phase, and has a structure similar to those of  $[\text{As}(\text{N}_3)_6]^-$ ,<sup>[28]</sup>  $[\text{Sb}(\text{N}_3)_6]^-$ ,<sup>[27]</sup>  $[\text{Si}(\text{N}_3)_6]^-$ ,<sup>[38]</sup>  $[\text{Ge}(\text{N}_3)_6]^-$ ,<sup>[39]</sup> and  $[\text{Ti}(\text{N}_3)_6]^{2-}$ ,<sup>[1]</sup> but contrary to that of  $[\text{Te}(\text{N}_3)_6]^{2-}$ <sup>[40]</sup> which contains a sterically active free valence electron pair on its central atom. The average Nb–N bond length in  $[\text{Nb}(\text{N}_3)_6]^-$  (2.027 Å) is larger than that found for  $[\text{Nb}(\text{N}_3)_5(\text{CH}_3\text{CN})]$  (1.997 Å), as expected from the formal negative charge in the

**Table 2:** Comparison of observed and unscaled calculated vibrational frequencies [ $\text{cm}^{-1}$ ] and intensities for  $[\text{Nb}(\text{N}_3)_6]^{-}$  in point group  $S_6$ .

	Description	IR	Observed	Calculated <sup>[b]</sup> (IR) [Raman]	
			Raman <sup>[c]</sup>	B3LYP/SBKJ + (d)	MP2/SBKJ + (d)
$A_g$	$\nu_1$	$\nu_{as}\text{N}_3$	2131 (10.0) 2112 (5.6)	2218 (0) [1428]	2129 (0) [1388]
	$\nu_2$	$\nu_s\text{N}_3$	1342 (2.0)	1432 (0) [49]	1283 (0) [60]
	$\nu_3$	$\delta\text{N}_3$	616 (2.8)	588 (0) [8.8]	565 (0) [39]
	$\nu_4$	$\delta\text{N}_3$		580 (0) [2.2]	524 (0) [2.3]
	$\nu_5$	$\nu_s\text{NbN}_6$	433 (5.3) 414 (4.8)	401 (0) [147]	402 (0) [367]
	$\nu_6$	$\delta_s\text{NbN}_6$	225 (3.5)	249 (0) [13]	242 (0) [51]
	$\nu_7$	$\tau$		74 (0) [14]	72 (0) [31]
	$\nu_8$	$\tau$		34 (0) [37]	32 (0) [39]
$E_g$	$\nu_9$	$\nu_{as}\text{N}_3$	2080 (2.1) 2060 (2.3)	2164 (0) [1063]	2146 (0) [110]
	$\nu_{10}$	$\nu_s\text{N}_3$		1413 (0) [50]	1279 (0) [154]
	$\nu_{11}$	$\delta\text{N}_3$		582 (0) [8.4]	550 (0) [73]
	$\nu_{12}$	$\delta\text{N}_3$		580 (0) [0.63]	521 (0) [4.2]
	$\nu_{13}$	$\nu_s\text{NbN}_6$	339 (2.7)	334 (0) [12]	350 (0) [38]
	$\nu_{14}$	$\delta_s\text{NbN}_6$	217 (3.5)	238 (0) [34]	234 (0) [31]
	$\nu_{15}$	$\tau$		87 (0) [36]	89 (0) [92]
	$\nu_{16}$	$\tau$		36 (0) [69]	38 (0) [80]
$A_u$	$\nu_{17}$	$\nu_{as}\text{N}_3$	2121 s 2080 vs	2185 (4084) [0]	2152 (2577) [0]
	$\nu_{18}$	$\nu_s\text{N}_3$	1336 ms	1406 (677) [0]	1271 (338) [0]
	$\nu_{19}$	$\delta\text{N}_3$	640 vw	580 (0.91) [0]	549 (100) [0]
	$\nu_{20}$	$\delta\text{N}_3$	624 w	574 (49) [0]	505 (8.0) [0]
	$\nu_{21}$	$\nu_{as}\text{NbN}_6$	409 mw	400 (536) [0]	418 (629) [0]
	$\nu_{22}$	$\delta_{as}\text{NbN}_6$		276 (15) [0]	262 (31) [0]
	$\nu_{23}$	$\tau\text{NbN}_6$		140 (2.8) [0]	114 (0.48) [0]
	$\nu_{24}$	$\tau$		27 (0.006) [0]	29 (0.022) [0]
$E_u$	$\nu_{25}$	$\tau$		24 (1.6) [0]	14 (0.37) [0]
	$\nu_{26}$	$\nu_{as}\text{N}_3$	2069 vs 2060 vs	2170 (4366) [0]	2141 (2681) [0]
	$\nu_{27}$	$\nu_s\text{N}_3$	1361 m 1351 m	1409 (739) [0]	1278 (314) [0]
	$\nu_{28}$	$\delta\text{N}_3$	600 w	577 (126) [0]	544 (94) [0]
	$\nu_{29}$	$\delta\text{N}_3$	583 vw	570 (38) [0]	502 (8.2) [0]
	$\nu_{30}$	$\nu_{as}\text{NbN}_6$	409 mw	391 (874) [0]	404 (1045) [0]
	$\nu_{31}$	$\delta_{as}\text{NbN}_6$		233 (26) [0]	223 (30) [0]
	$\nu_{32}$	$\delta_{\text{wag/rock}}\text{NbN}_6$	151 (4.3)	154 (13) [0]	128 (31) [0]
	$\nu_{33}$	$\tau$		36 (4.8) [0]	38 (3.1) [0]
	$\nu_{34}$	$\tau$		15 (1.6) [0]	6 (1.9) [0]

[a] Calculated IR and Raman intensities are given in  $\text{kmol}^{-1}$  and  $\text{\AA}^4\text{amu}^{-1}$ , respectively; observed spectra are for the solid  $[\text{P}(\text{C}_6\text{H}_5)_4]^+$  salt. [b] Values shown in parentheses and square brackets are the respective IR and Raman intensities. [c] Intensities shown in parentheses.

former, which increases the ionic character of the azido ligands. The relatively large variation in the Nb-N-N bond angles in  $[\text{Nb}(\text{N}_3)_6]^{-}$ , which range from 131.7 to 156.2°, is attributed to intramolecular repulsion effects among the ligands.

In summary, this paper reports the synthesis and characterization of the first examples of binary Group 5 azides and provides the first experimental proof for the existence of linear M-N-N coordination for azido ligands.

## Experimental Section

**Caution!** Covalent azido compounds are potentially hazardous and can decompose explosively under various conditions! The polyazido

compounds of this work are extremely shock-sensitive and can explode violently upon the slightest provocation. They should be handled only on a scale of less than 1 mmol. Because of the high energy content and high detonation velocities of these azides, their explosions are particularly violent and can cause, even on a 1-mmol scale, significant damage. The use of appropriate safety precautions (safety shields, face shields, leather gloves, protective clothing, such as heavy leather welding suits, and ear plugs) is mandatory. Teflon containers should be used, whenever possible, to avoid hazardous shrapnel formation. The manipulation of these materials is facilitated by handling them, whenever possible, in solution to avoid detonation propagation, by the use of large inert counterions as spacers, and by anion formation, which increases the partial negative charge on the terminal  $\text{N}_\gamma$  atoms and thereby reduces the  $\text{N}_\beta\text{--N}_\gamma$  triple-bond character and strengthens the weak  $\text{N}_\alpha\text{--N}_\beta$  single bond. **Ignoring safety precautions can lead to serious injuries!**

**Materials and Apparatus:** All reactions were carried out in teflon-FEP ampoules that were closed by stainless steel valves. Volatile materials were handled in a Pyrex glass or stainless steel/teflon-FEP vacuum line.<sup>[41]</sup> All reaction vessels were passivated with  $\text{ClF}_3$  prior to use. Nonvolatile materials were handled in the dry argon atmosphere of a glovebox.

Raman spectra were recorded directly in the teflon reactors in the range 3600–80  $\text{cm}^{-1}$  on a Bruker Equinox 55 FT-RA spectrophotometer by using a Nd-YAG laser at 1064 nm with power levels less than 50 mW. Infrared spectra were recorded in the range 4000–400  $\text{cm}^{-1}$  on a Midac M Series FT-IR spectrometer by using KBr pellets. The pellets were prepared inside the glovebox with an Econo minipress (Barnes Engineering Co.) and transferred in a closed container to the

spectrometer before placing them quickly into the sample compartment, which was purged with dry nitrogen to minimize exposure to atmospheric moisture and potential hydrolysis of the sample.

The starting materials  $\text{NbF}_5$ ,  $\text{TaF}_5$  (both Ozark Mahoning), and  $[\text{P}(\text{C}_6\text{H}_5)_4]\text{I}$  (Aldrich) were used without further purification.  $(\text{CH}_3)_3\text{SiN}_3$  (Aldrich) was purified by fractional condensation prior to use. Solvents were dried by standard methods and freshly distilled prior to use.  $[\text{P}(\text{C}_6\text{H}_5)_4]\text{N}_3$  and  $[\text{P}(\text{C}_6\text{H}_5)_4]\text{F}$  were prepared from  $[\text{P}(\text{C}_6\text{H}_5)_4]\text{I}$  and stoichiometric amounts of  $\text{AgN}_3$  and  $\text{AgF}$ , respectively, in aqueous solution and separated from the precipitated  $\text{AgI}$  by filtration.

$[\text{M}(\text{N}_3)_5]$  ( $\text{M} = \text{Nb}, \text{Ta}$ ): A sample of  $\text{NbF}_5$  (0.55 mmol) or  $\text{TaF}_5$  (0.59 mmol) was loaded into a teflon-FEP ampoule, and  $\text{SO}_2$  (1 g) and  $(\text{CH}_3)_3\text{SiN}_3$  (5.5 mmol) were added in vacuo at  $-196^\circ\text{C}$ . The mixture was warmed to  $-30^\circ\text{C}$ . After 2 h, the temperature was raised to

–20 °C, and all volatile material was removed in vacuum, leaving behind solid  $[\text{M}(\text{N}_3)_5]$ .

$[\text{Nb}(\text{N}_3)_5]$ : Mass of isolated material: 0.175 g; calcd for 0.55 mmol: 0.166 g. Raman (–80 °C):  $\tilde{\nu}$  [intensity in  $\text{\AA}^4\text{amu}^{-1}$ ]: 2155 [10.0], 2106 [5.5] ( $\nu_{\text{as}} \text{N}_3$ ), 1385 [1.6] ( $\nu_{\text{s}} \text{N}_3$ ), 628 [0.7], 590 sh ( $\delta \text{N}_3$ ), 427 sh ( $\nu_{\text{as}} \text{NbN}_3$  eq), 413 [3.2] ( $\nu_{\text{s}} \text{NbN}_3$  eq), 360 sh ( $\nu_{\text{s}} \text{NbN}_2$  ax), 288 [0.7] ( $\delta_{\text{sciss}} \text{NbN}_3$  eq), 234  $\text{cm}^{-1}$  [0.7], ( $\rho \text{NbN}_2$  ax); IR (KBr):  $\tilde{\nu}$  = 2124 vs, 2088 vs ( $\nu_{\text{as}} \text{N}_3$ ), 1374 m, 1347 s ( $\nu_{\text{s}} \text{N}_3$ ), 591 mw, 569 w ( $\delta \text{N}_3$ ), 450 sh ( $\nu_{\text{as}} \text{NbN}_3$  eq), 440 mw ( $\nu_{\text{as}} \text{NbN}_2$  ax), 422  $\text{cm}^{-1}$  w ( $\nu_{\text{s}} \text{NbN}_3$  eq); ax = axial, eq = equatorial.

$[\text{Ta}(\text{N}_3)_5]$ : Mass of isolated material: 0.247 g; calcd for 0.59 mmol: 0.231 g. Raman (–80 °C):  $\tilde{\nu}$  [intensity in  $\text{\AA}^4\text{amu}^{-1}$ ]: 2182 [10.0], 2129 [3.3] ( $\nu_{\text{as}} \text{N}_3$ ), 623 [1.1], 590 sh ( $\delta \text{N}_3$ ), 450 sh ( $\nu_{\text{as}} \text{TaNa}_3$  eq), 426 [2.5] ( $\nu_{\text{s}} \text{TaNa}_3$  eq), 390 sh ( $\nu_{\text{s}} \text{TaNa}_2$  ax), 256 [1.7] ( $\delta_{\text{sciss}} \text{TaNa}_3$  eq), 221  $\text{cm}^{-1}$  [2.0] ( $\rho \text{TaNa}_2$  ax); IR (KBr):  $\tilde{\nu}$  = 2141 vs, 2103 vs ( $\nu_{\text{as}} \text{N}_3$ ), 1403 ms, 1364 m ( $\nu_{\text{s}} \text{N}_3$ ), 613 mw, 578 w ( $\delta \text{N}_3$ ), 410  $\text{cm}^{-1}$  mw ( $\nu_{\text{as}} \text{TaNa}_2$  ax).

In addition to the bands listed above, the following weak IR bands were observed which are attributed to overtones or combination bands:  $[\text{Nb}(\text{N}_3)_5]$ : 1667 w, 1263 w, 1195 sh, 1176 w, 1037 vw, 696 w, 660  $\text{cm}^{-1}$  w;  $[\text{Ta}(\text{N}_3)_5]$ : 1669 w, 1508 vw, 1274 sh, 1252 w, 1203 w, 1180 sh, 1036 vw, 850 w, 712 w, 683  $\text{cm}^{-1}$  w.

$[\text{M}(\text{N}_3)_5(\text{CH}_3\text{CN})]$  (M = Nb, Ta):  $\text{NbF}_5$  (0.39 mmol) or  $\text{TaF}_5$  (0.37 mmol) was loaded into a teflon-FEP ampoule, and  $\text{CH}_3\text{CN}$  (2 mL) and  $(\text{CH}_3)_3\text{SiN}_3$  (3.7 mmol) were added in vacuo at –196 °C. The mixture was warmed to –20 °C. After 2 h, all volatile material was removed in a vacuum at this temperature, leaving behind solid  $[\text{M}(\text{N}_3)_5(\text{CH}_3\text{CN})]$ .

$[\text{Nb}(\text{N}_3)_5(\text{CH}_3\text{CN})]$ : Mass of isolated material: 0.129 g; calcd for 0.39 mmol: 0.136 g. Raman (–80 °C):  $\tilde{\nu}$  [intensity in  $\text{\AA}^4\text{amu}^{-1}$ ]: 2928 [1.8] ( $\nu_{\text{s}} \text{CH}_3$ ), 2315 [1.2], 2289 [1.1] ( $\nu \text{CN}$ ), 2140 [10.0], 2121 [1.5], 2097 [1.9], 2090 [1.6], 2074 [2.2], 2058 [1.4] ( $\nu_{\text{as}} \text{N}_3$ ), 1415 [1.3], 1363 [1.2], 1351 [1.1], 1331 [1.1] ( $\delta \text{CH}_3$ ) and ( $\nu_{\text{s}} \text{N}_3$ ), 947 [1.0] ( $\nu \text{CC}$ ), 620 [1.2], 610 [1.0], 599 [1.2], 580 [1.1], 566 [1.0], 557 [1.1] ( $\delta \text{N}_3$ ), 441 [3.1], 435 [2.8], 423 [1.7], 419 [1.7], 411 [2.0] ( $\nu \text{NbN}_x$ ), 281 [1.1], 266 [1.3], 256 [1.3], 248 [1.3], 226 [1.6] ( $\delta \text{NbN}_x$ ), 189 [1.3], 180 [1.3], 139 [1.6], 96 [2.9] (torsional modes).

$[\text{Ta}(\text{N}_3)_5(\text{CH}_3\text{CN})]$ : Mass of isolated material: 0.175 g; calcd for 0.37 mmol: 0.161 g. Raman (–80 °C):  $\tilde{\nu}$  [intensity in  $\text{\AA}^4\text{amu}^{-1}$ ]: 2933 [1.7] ( $\nu_{\text{s}} \text{CH}_3$ ), 2319 [0.5], 2291 [0.5] ( $\nu \text{CN}$ ), 2172 [10.0], 2162 [1.2], 2123 [1.2], 2103 [1.1] ( $\nu_{\text{as}} \text{N}_3$ ), 1389 [0.4], 1361 [0.4] ( $\delta \text{CH}_3$ ) and ( $\nu_{\text{s}} \text{N}_3$ ), 948 [1.0] ( $\nu \text{CC}$ ), 592 [0.3] ( $\delta \text{N}_3$ ), 438 [2.1], 417 [0.6] ( $\nu \text{NbN}_x$ ), 250 [0.7], 266 [1.3], 226 [0.6] ( $\delta \text{NbN}_x$ ), 192 [0.9] (torsional mode).

$[\text{P}(\text{C}_6\text{H}_5)_4][\text{M}(\text{N}_3)_6]$  (M = Nb, Ta): Neat  $[\text{P}(\text{C}_6\text{H}_5)_4]\text{N}_3$  (0.25 mmol) was added to a frozen solution of  $[\text{M}(\text{N}_3)_5]$  (0.25 mmol) in  $\text{CH}_3\text{CN}$  (15 mmol) at –78 °C. The reaction mixture was warmed to –25 °C and occasionally agitated. After 2 h, all volatiles were removed at ambient temperature in a dynamic vacuum, leaving behind solid  $[\text{P}(\text{C}_6\text{H}_5)_4][\text{M}(\text{N}_3)_6]$ .

$[\text{P}(\text{C}_6\text{H}_5)_4][\text{Nb}(\text{N}_3)_6]$ : Orange solid. Mass of isolated material: 0.160 g; calcd for 0.25 mmol: 0.171 g. The IR and Raman bands of  $[\text{Nb}(\text{N}_3)_6]^-$  are given in Table 2.

$[\text{P}(\text{C}_6\text{H}_5)_4][\text{Ta}(\text{N}_3)_6]$ : Pale yellow solid. Mass of isolated material 0.207 g; calcd for 0.25 mmol: 0.193 g. Raman bands from  $[\text{Ta}(\text{N}_3)_6]^-$  (–80 °C):  $\tilde{\nu}$  [intensity in  $\text{\AA}^4\text{amu}^{-1}$ ]: 2159 [10.0], 2111 [1.0], 2103 [1.0], 2091 [0.8], 2081 [0.7] ( $\nu_{\text{as}} \text{N}_3$ ), 1355 [0.8] ( $\nu_{\text{s}} \text{N}_3$ ), 609 [0.6], 582 [0.4] ( $\delta \text{N}_3$ ), 437 [2.8], 372 [0.7], 364 [0.8], 353 [0.8] ( $\nu \text{TaNa}_6$ ), 225 [1.8], 215 [1.8] ( $\delta \text{TaNa}_6$ ), 168 [2.6], 160  $\text{cm}^{-1}$  [2.6] (torsions); IR bands from  $[\text{Ta}(\text{N}_3)_6]^-$  (KBr):  $\tilde{\nu}$  = 2124 vs, 2113 vs, 2096 vs, 2087 vs ( $\nu_{\text{as}} \text{N}_3$ ), 1383 m, 1372 m, 1360 ms, 1348 s ( $\nu_{\text{s}} \text{N}_3$ ), 648 vw, 615 m, 600 mw, 585 mw, 576 w ( $\delta \text{N}_3$ ), 433 w, 418 mw, 414  $\text{cm}^{-1}$  mw ( $\nu \text{TaNa}_6$ ).

Theoretical Methods: The molecular structures, harmonic vibrational frequencies, and IR and Raman vibrational intensities were calculated by using second-order perturbation theory (MP2, also known as MBPT(2)<sup>[24]</sup>) and also at the DFT level by using the B3LYP hybrid functional,<sup>[23a]</sup> which included the VWN5 correlation functional.<sup>[23b]</sup> The Stevens, Basch, Krauss, and Jasien (SBKJ) effective core potentials and the corresponding valence-only basis sets were

used.<sup>[25a]</sup> The SBKJ valence basis set for nitrogen was augmented with a d-polarization function<sup>[25b]</sup> and a diffuse s + p shell,<sup>[25c]</sup> denoted as SBKJ + (d). Hessians (energy second derivatives) were calculated for the final equilibrium structures to verify them as local minima, that is, having a positive definite Hessian. All calculations were performed by using the electronic structure code GAMESS.<sup>[42]</sup>

Received: March 17, 2006

Published online: June 23, 2006

**Keywords:** azides · density functional calculations · niobium · tantalum · vibrational spectroscopy

- [1] R. Haiges, J. A. Boatz, S. Schneider, T. Schroer, K. O. Christe, *Angew. Chem.* **2004**, *116*, 3210; *Angew. Chem. Int. Ed.* **2004**, *43*, 3148.
- [2] R. Haiges, J. A. Boatz, R. Bau, S. Schneider, T. Schroer, M. Yousufuddin, K. O. Christe, *Angew. Chem.* **2005**, *117*, 1894; *Angew. Chem. Int. Ed.* **2005**, *44*, 1860.
- [3] A. Kornath, *Angew. Chem.* **2001**, *113*, 3231; *Angew. Chem. Int. Ed.* **2001**, *40*, 3135, and references therein.
- [4] K. Dehnicke, J. Strähle, *Z. Anorg. Allg. Chem.* **1965**, *338*, 287.
- [5] K. Dehnicke, *J. Inorg. Nucl. Chem.* **1965**, *27*, 809.
- [6] J. Strähle, *Z. Anorg. Allg. Chem.* **1974**, *405*, 139.
- [7] R. Choukroun, D. Gervais, *J. Chem. Soc. Dalton Trans.* **1980**, 1800.
- [8] U. Müller, R. Dübgen, K. Dehnicke, *Z. Anorg. Allg. Chem.* **1981**, *473*, 115.
- [9] a) W. Beck, E. Schuierer, P. Poellmann, W. P. Fehlhammer, *Z. Naturforsch. B* **1966**, *21*, 811; b) W. Beck, W. P. Fehlhammer, P. Poellmann, E. Schuierer, K. Feldt, *Chem. Ber.* **1967**, *100*, 2335.
- [10] D. B. Sable, W. H. Armstrong, *Inorg. Chem.* **1992**, *31*, 161.
- [11] J. H. Espenson, J. R. Pladziewicz, *Inorg. Chem.* **1970**, *9*, 1380.
- [12] M. Kasper, R. Bereman, *Inorg. Nucl. Chem. Lett.* **1974**, *10*, 443.
- [13] M. Herberhold, A.-M. Dietel, W. Milius, *Z. Anorg. Allg. Chem.* **1999**, *625*, 1885.
- [14] J. H. Osborne, A. L. Rheingold, W. C. Troglor, *J. Am. Chem. Soc.* **1985**, *107*, 7945.
- [15] M. Herberhold, A. Goller, W. Milius, *Z. Anorg. Allg. Chem.* **2003**, *629*, 1162.
- [16] M. Herberhold, A. Goller, W. Milius, *Z. Anorg. Allg. Chem.* **2003**, *629*, 1557.
- [17] M. Herberhold, A. Goller, W. Milius, *Z. Anorg. Allg. Chem.* **2001**, *627*, 891.
- [18] J. H. Meyer, *Z. Anorg. Allg. Chem.* **1995**, *621*, 921.
- [19] O. Reckeweg, H.-J. Meyer, A. Simon, *Z. Anorg. Allg. Chem.* **2002**, *628*, 920.
- [20] H.-J. Meyer, *Z. Anorg. Allg. Chem.* **1995**, *621*, 921.
- [21] R. Dübgen, U. Müller, F. Weller, K. Dehnicke, *Z. Anorg. Allg. Chem.* **1980**, *471*, 89.
- [22] A. M. Golub, H. Köhler, V. V. Stopenko, *Chemistry of Pseudo-halides*, Elsevier, Amsterdam, **1986**.
- [23] a) A. D. Becke, *J. Chem. Phys.* **1993**, *98*, 5648; P. J. Stephens, F. J. Devlin, C. F. Chabrowski, M. J. Frisch, *J. Phys. Chem.* **1994**, *98*, 11623; R. H. Hertwig, W. Koch, *Chem. Phys. Lett.* **1997**, *268*, 345; b) S. H. Vosko, L. Wilk, M. Nusair, *Can. J. Phys.* **1980**, *58*, 1200.
- [24] C. Moller, M. S. Plesset, *Phys. Rev.* **1934**, *46*, 618; J. A. Pople, J. S. Binkley, R. Seeger, *Int. J. Quantum Chem. Symp.* **1976**, *10*, 1; M. J. Frisch, M. Head-Gordon, J. A. Pople, *Chem. Phys. Lett.* **1990**, *166*, 275; R. J. Bartlett, D. M. Silver, *Int. J. Quantum Chem. Symp.* **1975**, *9*, 1927.
- [25] a) W. J. Stevens, H. Basch, M. Krauss, *J. Chem. Phys.* **1984**, *81*, 6026; W. J. Stevens, M. Krauss, H. Basch, P. G. Jasien, *Can. J. Chem.* **1992**, *70*, 612; b) P. C. Hariharan, J. A. Pople, *Theor.*

- Chim. Acta* **1973**, 28, 213; c) T. Clark, J. Chandrasekhar, G. W. Spitznagel, P. von R. Schleyer, *J. Comput. Chem.* **1983**, 4, 294.
- [26] J. Drummond, J. S. Wood, *Chem. Commun.* **1969**, 1373.
- [27] R. Haiges, J. A. Boatz, A. Vij, V. Vij, M. Gerken, S. Schneider, T. Schroer, M. Yousufuddin, K. O. Christe, *Angew. Chem.* **2004**, 116, 6844; *Angew. Chem. Int. Ed.* **2004**, 43, 6676.
- [28] a) K. Karaghiosoff, T. M. Klapötke, B. Krumm, H. Nöth, T. Schütt, M. Suter, *Inorg. Chem.* **2002**, 41, 170; b) T. M. Klapötke, H. Nöth, T. Schütt, M. Warchhold, *Angew. Chem.* **2000**, 112, 2197; *Angew. Chem. Int. Ed.* **2000**, 39, 2108.
- [29] a) R. J. Gillespie, I. Hargittai, *The VSEPR Model of Molecular Geometry*, Allyn and Bacon, Needham Heights, MA, **1991**; b) R. J. Gillespie, P. L. A. Popelier, *Chemical Bonding and Molecular Geometry: from Lewis to Electron Densities*, Oxford University Press, Oxford, **2001**.
- [30] L. Gagliardi, P. Pyykkö, *Inorg. Chem.* **2003**, 42, 3074.
- [31] M. Teichert, J. A. Boatz, personal communication.
- [32] P. H. Bird, M. R. Churchill, *J. Chem. Soc. Chem. Commun.* **1967**, 403.
- [33] Crystal data for  $C_2H_3N_{16}Nb$ :  $M_r = 344.11$ , monoclinic, space group  $P2_1/c$ ,  $a = 7.9805(12)$ ,  $b = 10.4913(16)$ ,  $c = 14.695(2)$  Å,  $\alpha = 90$ ,  $\beta = 96.353(2)$ ,  $\gamma = 90^\circ$ ,  $V = 1222.8(3)$  Å<sup>3</sup>,  $F(000) = 672$ ,  $\rho_{\text{calcd}} = 1.869$  g cm<sup>-3</sup>,  $Z = 4$ ,  $\mu = 1.004$  mm<sup>-1</sup>, approximate crystal dimensions  $0.25 \times 0.08 \times 0.02$  mm<sup>3</sup>,  $\theta = 2.39$  to  $27.48^\circ$ ,  $Mo_{K\alpha}$  ( $\lambda = 0.71073$  Å),  $T = 163(2)$  K, 3392 measured data (Bruker 3-circle, SMART APEX CCD with  $\chi$ -axis fixed at  $54.74^\circ$  using the SMART V 5.625 program, Bruker AXS: Madison, WI, 2001), of which 839 ( $R_{\text{int}} = 0.0204$ ) were unique. Lorentz and polarization correction (SAINT V 6.22 program, Bruker AXS: Madison, WI, **2001**), absorption correction (SADABS program, Bruker AXS: Madison, WI, **2001**). Structure solution by direct methods (SHELXTL 5.10, Bruker AXS: Madison, WI, **2000**), full-matrix least-squares refinement on  $F^2$ , data-to-parameters ratio: 15.9:1, final  $R$  indices [ $I > 2\sigma(I)$ ]:  $R1 = 0.0341$ ,  $wR2 = 0.0692$ ,  $R$  indices (all data):  $R1 = 0.0546$ ,  $wR2 = 0.0746$ , GOF on  $F^2 = 1.003$ . CCDC-246594 contains the supplementary crystallographic data for  $[Nb(N_3)_5(CH_3CN)]$ . These data can be obtained free of charge from The Cambridge Crystallographic Data Centre via [www.ccdc.cam.ac.uk/data\\_request/cif](http://www.ccdc.cam.ac.uk/data_request/cif).
- [34] B. v. Ahlsen, B. Bley, S. Proemmel, R. Wartchow, H. Willner, F. Aubke, *Z. Anorg. Allg. Chem.* **1998**, 624, 1225.
- [35] a) D. M. Byler, D. F. Shriver, *Inorg. Chem.* **1973**, 12, 1412; b) D. M. Byler, D. F. Shriver **1974**, 13, 2697.
- [36] Crystal data for  $C_{24}H_{20}N_{18}NbP$ :  $M_r = 684.46$ , orthorhombic, space group  $P2_12_12$ ,  $a = 18.480(3)$ ,  $b = 23.153(4)$ ,  $c = 6.7831(13)$  Å,  $\alpha = 90$ ,  $\beta = 90$ ,  $\gamma = 90^\circ$ ,  $V = 2902.3(9)$  Å<sup>3</sup>,  $F(000) = 1384$ ,  $\rho_{\text{calcd}} = 1.566$  g cm<sup>-3</sup>,  $Z = 4$ ,  $\mu = 0.521$  mm<sup>-1</sup>, approximate crystal dimensions  $0.33 \times 0.05 \times 0.04$  mm<sup>3</sup>,  $\theta = 1.41$  to  $27.51^\circ$ ,  $Mo_{K\alpha}$  ( $\lambda = 0.71073$  Å),  $T = 133(2)$  K, 17936 measured data (Bruker 3-circle, SMART APEX CCD with  $\chi$ -axis fixed at  $54.74^\circ$  using the SMART V 5.625 program, Bruker AXS: Madison, WI, **2001**), of which 6575 ( $R_{\text{int}} = 0.0597$ ) were unique. Lorentz and polarization correction (SAINT V 6.22 program, Bruker AXS: Madison, WI, **2001**), absorption correction (SADABS program, Bruker AXS: Madison, WI, **2001**). Structure solution by direct methods (SHELXTL 5.10, Bruker AXS: Madison, WI, **2000**), full-matrix least-squares refinement on  $F^2$ , data-to-parameters ratio: 16.5:1, final  $R$  indices [ $I > 2\sigma(I)$ ]:  $R1 = 0.0518$ ,  $wR2 = 0.0936$ ,  $R$  indices (all data):  $R1 = 0.0858$ ,  $wR2 = 0.1049$ , GOF on  $F^2 = 1.028$ . CCDC-251934 contains the supplementary crystallographic data for  $[P(C_6H_5)_4][Nb(N_3)_6]$ . These data can be obtained free of charge from The Cambridge Crystallographic Data Centre via [www.ccdc.cam.ac.uk/data\\_request/cif](http://www.ccdc.cam.ac.uk/data_request/cif).
- [37] J. Weidlein, U. Mueller, K. Dehnicke, *Schwingungsspektroskopie*, Georg Thieme, Stuttgart, **1982**, p. 102.
- [38] A. C. Filippou, P. Portius, G. Schnakenburg, *J. Am. Chem. Soc.* **2002**, 124, 12396.
- [39] A. C. Filippou, P. Portius, D. U. Neumann, K.-D. Wehrstedt, *Angew. Chem.* **2000**, 112, 4524; *Angew. Chem. Int. Ed.* **2000**, 39, 4333.
- [40] T. M. Klapötke, H. Nöth, T. Schuett, M. Warchhold, *Angew. Chem.* **2000**, 112, 2197; *Angew. Chem. Int. Ed.* **2000**, 39, 2108.
- [41] K. O. Christe, W. W. Wilson, C. J. Schack, R. D. Wilson, *Inorg. Synth.* **1986**, 24, 39.
- [42] M. W. Schmidt, K. K. Baldrige, J. A. Boatz, S. T. Elbert, M. S. Gordon, J. H. Jensen, S. Koseki, N. Matsunaga, K. A. Nguyen, S. J. Su, T. L. Windus, M. Dupuis, J. A. Montgomery, *J. Comput. Chem.* **1993**, 14, 1347.